

A tritopic carbanionic N-heterocyclic dicarbene and its homo- and heterometallic coinage metal complexes

Fan Zhang, Xiao-Ming Cao, Jiwei Wang, Jiajun Jiao, Yongming Huang,* Min Shi, Pierre Braunstein and Jun Zhang*

General Methods

Unless otherwise stated, all reactions and manipulations were performed using standard Schlenk techniques. All solvents were purified by distillation using standard methods. Commercially available reagents were used without further purification. NMR spectra were recorded by using a Bruker 400 MHz spectrometer. Chemical shifts are reported in ppm from tetramethylsilane with the solvent resonance as the internal standard (^1H NMR CDCl_3 : 7.26 ppm; ^{13}C NMR CDCl_3 : 77.0 ppm). Mass spectra were recorded on the HP-5989 instrument by EI/ESI methods. X-ray diffraction analyses were performed by using a Bruker APEX-II CCD X-ray diffractometer.

Compound **1** were prepared according to the literature method.¹

Preparation and characterization

Synthesis of the trigold complex **2**

A mixture of **1** (200 mg, 0.20 mmol) and PPh_3 (105 mg, 0.40 mmol) in DCE was stirred for 3 h. All volatiles were removed under vacuum, the resulting solid was dissolved in DCM, and the solution was filtered through a pad of Celite. Water (5 mL) was added to the filtrate and vigorously stirred for a few minutes, the organic phase was transferred to a test tube and then the solvents were evaporated. In a nitrogen-filled round-bottom flask, the crude product was washed twice with diethyl ether, then dissolved in THF (6 mL) and the solution was cooled to -78°C . KHMDS (1 M in THF, 220 μL , 1.1 equiv.) was added dropwise, and then $\text{AuCl}\cdot\text{SMe}_2$ (59 mg, 0.20 mmol) and triphenylphosphine (52 mg, 0.20 mmol) were added. After the mixture was stirred for 15 min at -78°C , the cooling bath was removed, and the solution was warmed to room temperature. After further stirring for 4 h at room temperature, all volatiles were evaporated in vacuo and the crude product was purified by column chromatography using silica gel (v/v, $\text{DCM}/\text{EtOH} = 20:1$) to afford the pure **2** as a yellow solid (200 mg, 55%). ^1H NMR (400 MHz, CDCl_3) $\delta = 7.58$ (t, $J = 7.4$ Hz, 1H, H_{Ar}), 7.49 (t, $J = 7.0$ Hz, 3H, H_{Ar}), 7.44 (t, $J = 7.8$ Hz, 2H, H_{Ar}), 7.41-7.30 (m, 18H, H_{Ar}), 7.30-7.27 (m, 2H, H_{Ar}), 7.26-7.21 (m, 7H, H_{Ar}), 7.19 (t, $J = 6.8$ Hz, 6H, H_{Ar}), 7.06 (dd, $J = 12.4, 7.6$ Hz, 6H, H_{Ar}), 6.83 (dd, $J = 12.8, 7.6$ Hz, 6H, H_{Ar}), 3.09-2.99 (m,

2H, $\underline{\text{CH}}(\text{CH}_3)_2$), 2.94-2.71 (m, 2H, $\underline{\text{CH}}(\text{CH}_3)_2$), 1.25 (d, $J = 6.8$ Hz, 6H, CH_3), 1.16 (d, $J = 6.8$ Hz, 6H, CH_3), 1.08 (t, $J = 6.6$ Hz, 12H, CH_3); ^{13}C NMR (100 MHz, CDCl_3) $\delta = 203.24$ (d, $^2J_{\text{C-P}} = 115.5$ Hz, $\text{N-C}(\text{Au})=\text{N}$), 200.77 (d, $^2J_{\text{C-P}} = 129.2$ Hz, $\text{C}=\underline{\text{C}}(\text{Au})-\text{N}$), 163.37 (d, $^2J_{\text{C-P}} = 117.4$ Hz, $\text{C}=\underline{\text{C}}(\text{Au})=\text{C}$), 160.24 (dd, $^3J_{\text{C-P}} = 6.4$ Hz, $^4J_{\text{C-P}} = 3.6$ Hz, $\underline{\text{C}}=\text{O}$), 145.45 (s, N-C_{Ar}), 145.34 (s, N-C_{Ar}), 143.71 (s, C_{Ar}), 137.44 (s, C_{Ar}), 133.92 (d, $^2J_{\text{C-P}} = 13.5$ Hz, PPh_3), 133.65 (d, $^2J_{\text{C-P}} = 13.8$ Hz, PPh_3), 133.42 (d, $^2J_{\text{C-P}} = 13.6$ Hz, PPh_3), 131.90 (s, C_{Ar}), 131.37 (s, C_{Ar}), 130.97 (s, C_{Ar}), 130.46 (s, C_{Ar}), 129.94 (s, C_{Ar}), 129.54 (s, C_{Ar}), 129.34 (s, C_{Ar}), 128.99 (d, $^2J_{\text{C-P}} = 11.6$ Hz, PPh_3), 128.88 (d, $^2J_{\text{C-P}} = 11.3$ Hz, PPh_3), 127.70 (s, C_{Ar}), 127.13 (s, C_{Ar}), 124.44 (s, C_{Ar}), 124.05 (s, C_{Ar}), 29.44 (s, $\underline{\text{CH}}(\text{CH}_3)_2$), 28.60 (s, $\underline{\text{CH}}(\text{CH}_3)_2$), 28.33 (s, $\underline{\text{CH}}(\text{CH}_3)_2$), 24.45 (s, CH_3), 24.40 (s, CH_3), 24.27 (s, CH_3), 23.94 (s, CH_3); ^{31}P NMR (162 MHz, CDCl_3) $\delta = 42.24$ (d, $J = 5.0$ Hz), 41.07 (d, $J = 4.7$ Hz), 38.55. Anal. calcd. for $\text{C}_{82}\text{H}_{79}\text{Au}_3\text{ClN}_2\text{OP}_3(1.5 \text{ CH}_2\text{Cl}_2)$: C, 51.29; H, 4.23; N, 1.43; found: C, 51.31; H, 4.61; N, 1.43; HRMS (MALDI): m/z $[\text{M-Cl}]^+$ calcd. for $\text{C}_{82}\text{H}_{79}\text{Au}_3\text{N}_2\text{OP}_3^+$: 1791.4396; found: 1791.4161.

Synthesis of the trinuclear gold-silver complex **3**

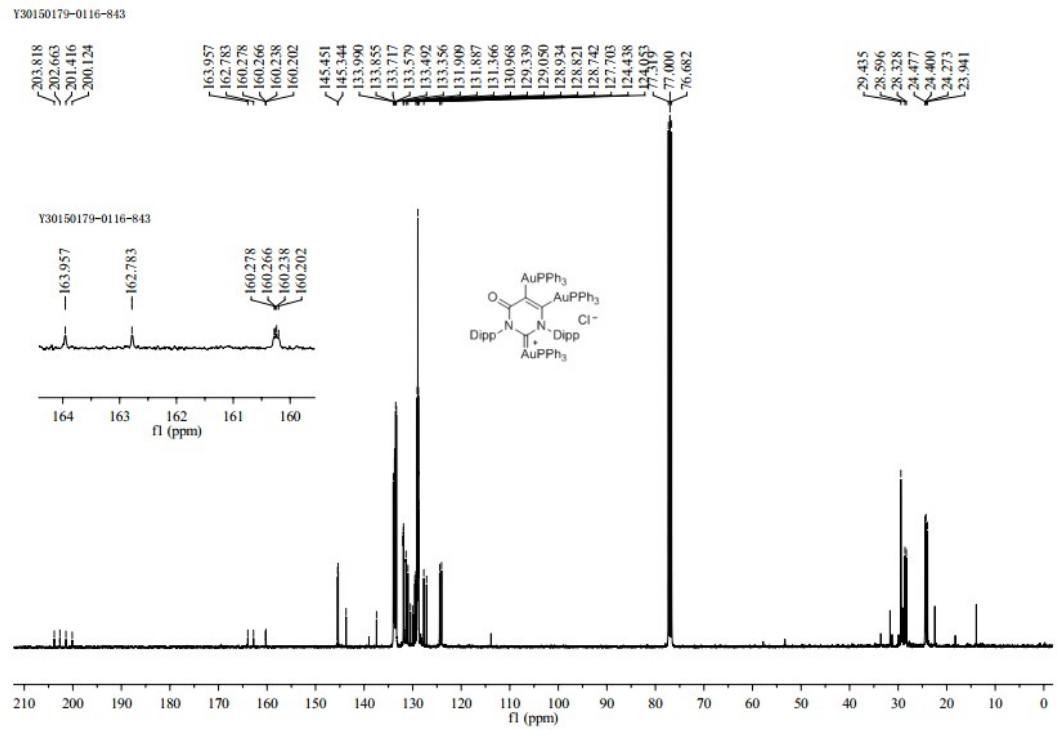
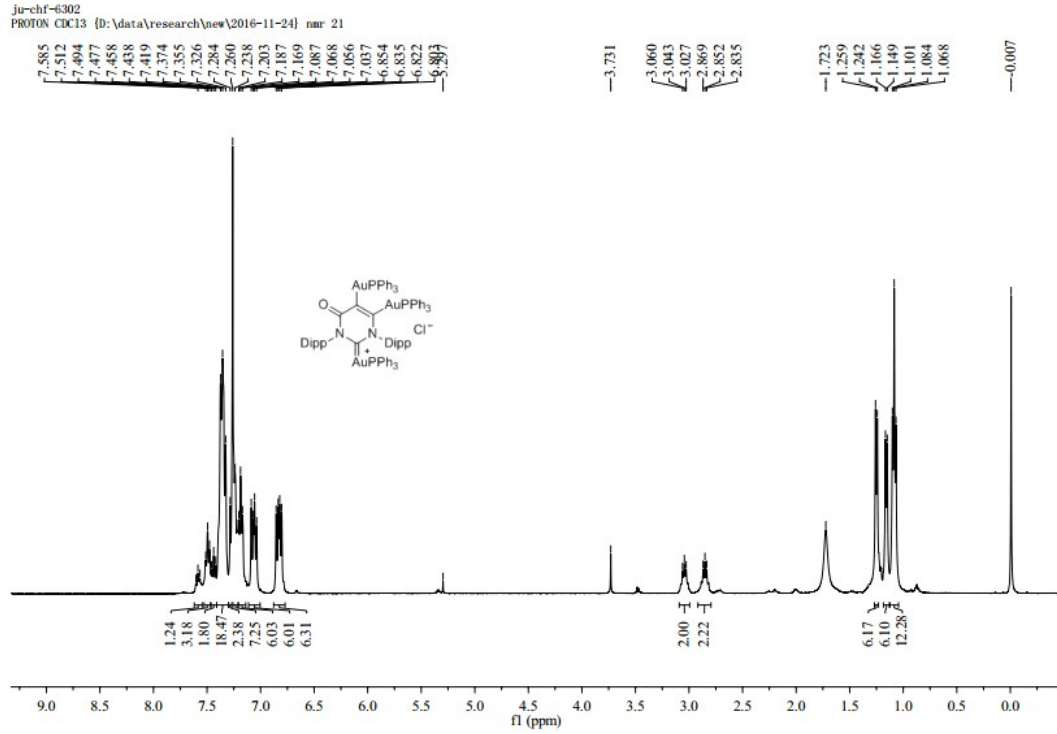
In a nitrogen-filled round-bottom flask, a solution of **1** (200 mg, 0.20 mmol) in THF (6 mL) was cooled to -78 °C, KHMDS (1 M in THF, 440 μL , 2.2 equiv.) was added dropwise and then $\text{AgOTf}(\text{PPh}_3)$ (208 mg, 0.40 mmol) was added. After the reaction mixture was stirred for 15 min at -78 °C, the cooling bath was removed, and the solution was warmed to room temperature. After 4 h at room temperature, all volatiles were evaporated in vacuo and the crude product was purified by column chromatography using silica gel (v/v, PE/EA = 3:1) to afford pure **3** as a yellow solid (212 mg, 72%). ^1H NMR (400 MHz, CDCl_3) $\delta = 7.54$ (t, $J = 6.6$ Hz, 1H, H_{Ar}), 7.44 (t, $J = 7.8$ Hz, 2H, H_{Ar}), 7.42-7.31 (m, 13H, H_{Ar}), 7.25-7.20 (m, 8H, H_{Ar}), 7.19-7.13 (m, 6H, H_{Ar}), 7.08 (dd, $J = 12.0, 7.2$ Hz, 6H, H_{Ar}), 3.13-3.05 (m, 2H, $\underline{\text{CH}}(\text{CH}_3)_2$), 2.94-2.85 (m, 2H, $\underline{\text{CH}}(\text{CH}_3)_2$), 1.31-1.22 (m, 18H, CH_3), 1.16 (d, $J = 6.4$ Hz, 6H, CH_3); ^{13}C NMR (100 MHz, CDCl_3) $\delta = 204.36$ (dd, $^1J_{\text{C-Ag}} = 253.0$ Hz, $J^{107\text{Ag}-109\text{Ag}} = 18.3$ Hz, $\text{N-C}(\text{Ag})=\text{N}$), 199.16 (d, $^2J_{\text{C-P}} = 128.9$ Hz, $\text{C}=\underline{\text{C}}(\text{Au})-\text{N}$), 161.24 (d, $^2J_{\text{C-P}} = 118.6$ Hz, $\text{C}=\underline{\text{C}}(\text{Au})-\text{C}$), 160.27 (dd, $^3J_{\text{C-P}} = 10.0$ Hz, $^4J_{\text{C-P}} = 4.1$ Hz, $\underline{\text{C}}=\text{O}$), 145.89 (s, C_{Ar}), 144.86 (s, N-C_{Ar}), 144.50 (s, N-C_{Ar}), 139.40 (s, C_{Ar}), 134.08 (d, $^2J_{\text{C-P}} = 13.6$ Hz, PPh_3), 133.83 (d, $^2J_{\text{C-P}} = 13.8$ Hz, PPh_3), 131.17 (s, C_{Ar}), 130.88 (s, C_{Ar}), 130.38 (s, C_{Ar}), 129.88 (s, C_{Ar}), 129.35 (s, C_{Ar}), 129.18 (s, C_{Ar}), 129.07 (s, C_{Ar}), 128.85 (d, $^4J_{\text{C-P}} = 3.8$ Hz, PPh_3), 128.74 (d, $^4J_{\text{C-P}} = 3.6$ Hz, PPh_3), 124.41 (s, C_{Ar}), 124.12 (s, C_{Ar}), 28.47 (s, $\underline{\text{CH}}(\text{CH}_3)_2$), 28.26 (s, $\underline{\text{CH}}(\text{CH}_3)_2$), 24.69 (s, CH_3), 24.59 (s, CH_3), 24.37 (s, CH_3), 24.33 (s, CH_3); ^{31}P NMR (162 MHz, CDCl_3) $\delta = 42.55$ (d, $J = 6.0$ Hz), 41.06 (dd, $J = 6.0, 3.4$ Hz). Anal. calcd. for $\text{C}_{64}\text{H}_{64}\text{AuClAgN}_2\text{OP}_2(0.5 \text{ CH}_2\text{Cl}_2)$: C, 51.00; H, 4.31; N, 1.84; found: C, 50.96; H, 4.30; N, 1.50.

Synthesis of the trinuclear gold-copper complex 4

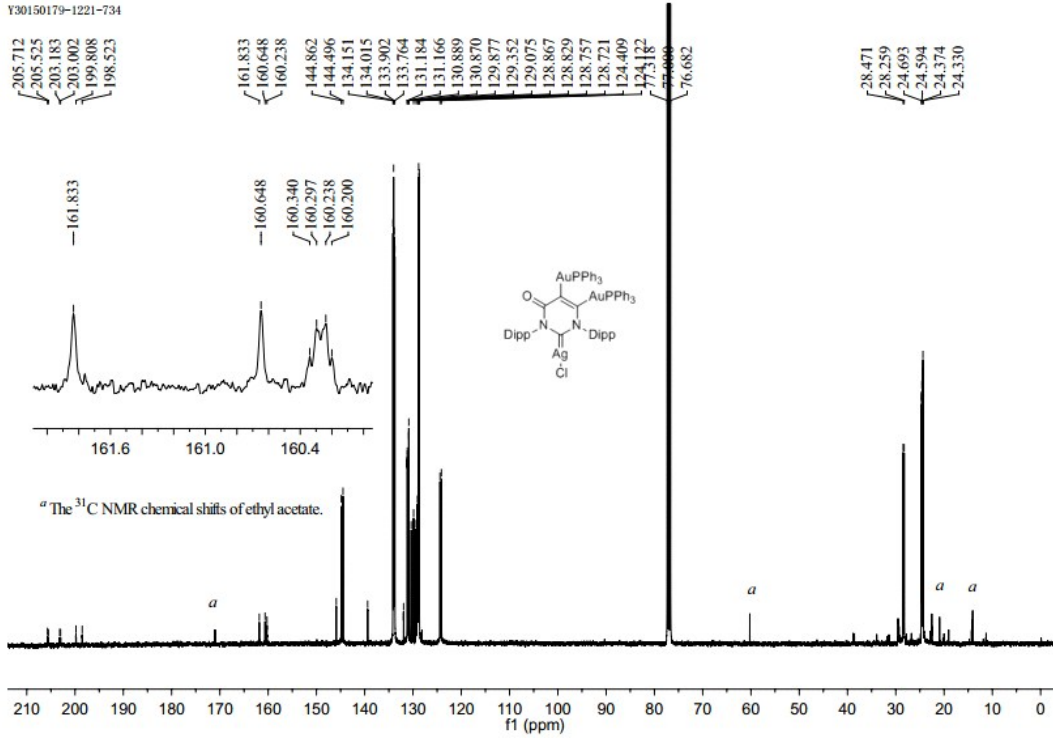
A mixture of **1** (200 mg, 0.20 mmol) and PPh₃ (105 mg, 0.40 mmol) in DCE was stirred for 3 h. All volatiles were removed under vacuum, the resulting solid was dissolved in DCM, and the solution was filtered through a pad of Celite. Water (5 mL) was added to the filtrate and the mixture was vigorously stirred for a few minutes, the organic phase was transferred to a test tube and then the solvents were evaporated. The crude product was washed twice with diethyl ether to afford a solid that was placed in a nitrogen-filled round-bottom flask, dissolved in THF (6 mL) and after the solution was cooled to -78 °C, KHMDS (1 M in THF, 220 μL, 1.1 equiv.) was added dropwise, then CuBr·SMe₂ (41 mg, 0.20 mmol) was added. After the mixture was stirred for 15 min at -78 °C, the cooling bath was removed, and the solution was warmed to room temperature. After 4 h at room temperature, all volatiles were evaporated in vacuo and the crude product was purified by column chromatography using silica gel (v/v, DCM/EtOH = 100:1) to afford pure **4** as a yellow solid (218 mg, 74%). ¹H NMR (400 MHz, CDCl₃) δ = 7.45 (t, *J* = 7.8 Hz, 1H, H_{Ar}), 7.42-7.30 (m, 13H, H_{Ar}), 7.25-7.19 (m, 10H, H_{Ar}), 7.19-7.13 (m, 6H, H_{Ar}), 7.12-7.04 (m, 6H, H_{Ar}), 3.13-3.04 (m, 2H, CH(CH₃)₂), 2.94-2.86 (m, 2H, CH(CH₃)₂), 1.29 (dd, *J* = 7.2, 5.2 Hz, 12H, CH₃), 1.24 (d, *J* = 6.8 Hz, 6H, CH₃), 1.16 (d, *J* = 6.8 Hz, 6H, CH₃); ¹³C NMR (100 MHz, CDCl₃) δ = 199.44 (d, ²*J*_{C-P} = 128.3 Hz, C=C(Au)-N), 198.57 (s, N-C(Cu)=N), 160.88 (d, ²*J*_{C-P} = 119.1 Hz, C=C(Au)-C), 160.53 (dd, ³*J*_{C-P} = 5.9 Hz, ⁴*J*_{C-P} = 3.8 Hz, C=O), 145.05 (s, N-C_{Ar}), 144.62 (s, N-C_{Ar}), 138.15 (s, C_{Ar}), 134.14 (d, ²*J*_{C-P} = 13.6 Hz, PPh₃), 131.15 (s, C_{Ar}), 131.01 (s, C_{Ar}), 130.50 (s, C_{Ar}), 130.00 (s, C_{Ar}), 129.48 (s, C_{Ar}), 128.86 (d, ⁴*J*_{C-P} = 4.2 Hz, PPh₃), 128.75 (d, ⁴*J*_{C-P} = 4.0 Hz, PPh₃), 124.25 (s, C_{Ar}), 123.97 (s, C_{Ar}), 29.56 (s, CH(CH₃)₂), 28.53 (s, CH(CH₃)₂), 28.30 (s, CH(CH₃)₂), 24.68 (s, CH₃), 24.59 (s, CH₃), 24.36 (s, CH₃); ³¹P NMR (162 MHz, CDCl₃) δ = 42.66 (d, *J* = 6.2 Hz), 41.16 (d, *J* = 6.2 Hz). Anal. calcd. for C₆₄H₆₄AuBrCuN₂OP₂: C, 52.06; H, 4.37; N, 1.90; found: C, 52.23; H, 4.17; N, 1.43.

NMR Spectra:

Complex 2

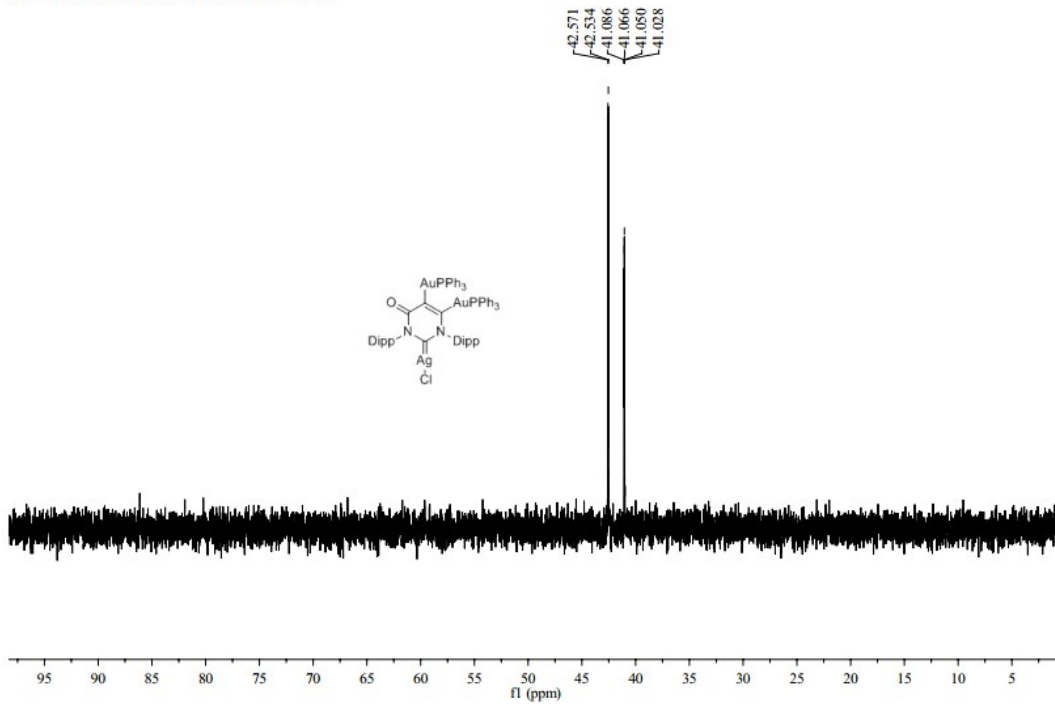


Y30150179-1221-734

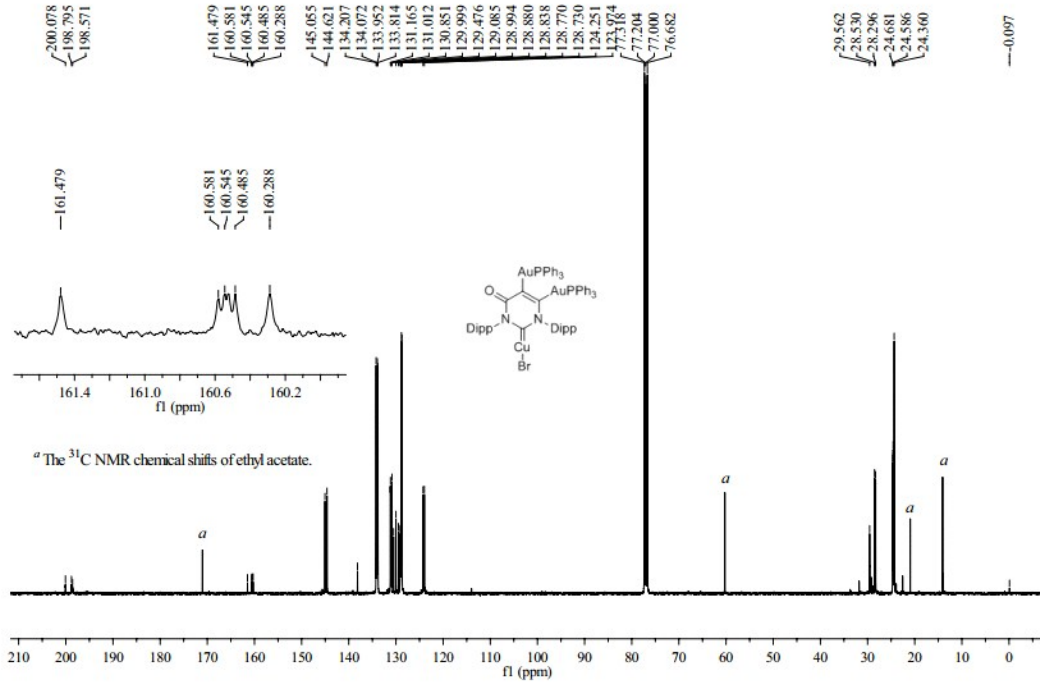
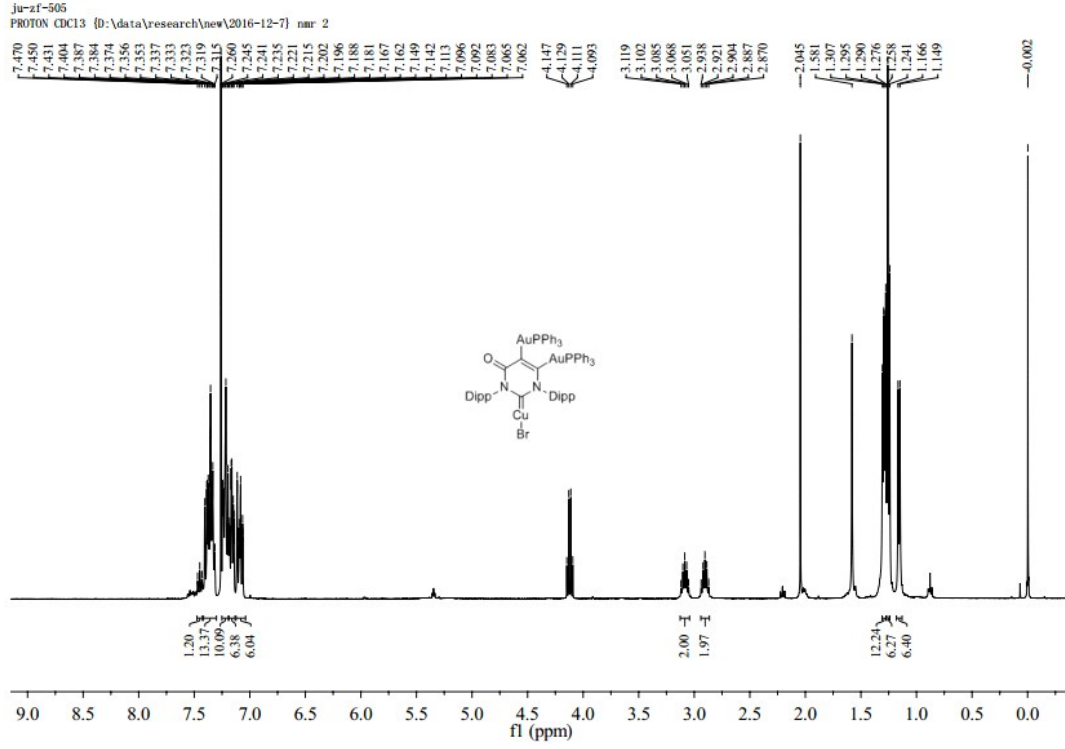


^a The ³¹C NMR chemical shifts of ethyl acetate.

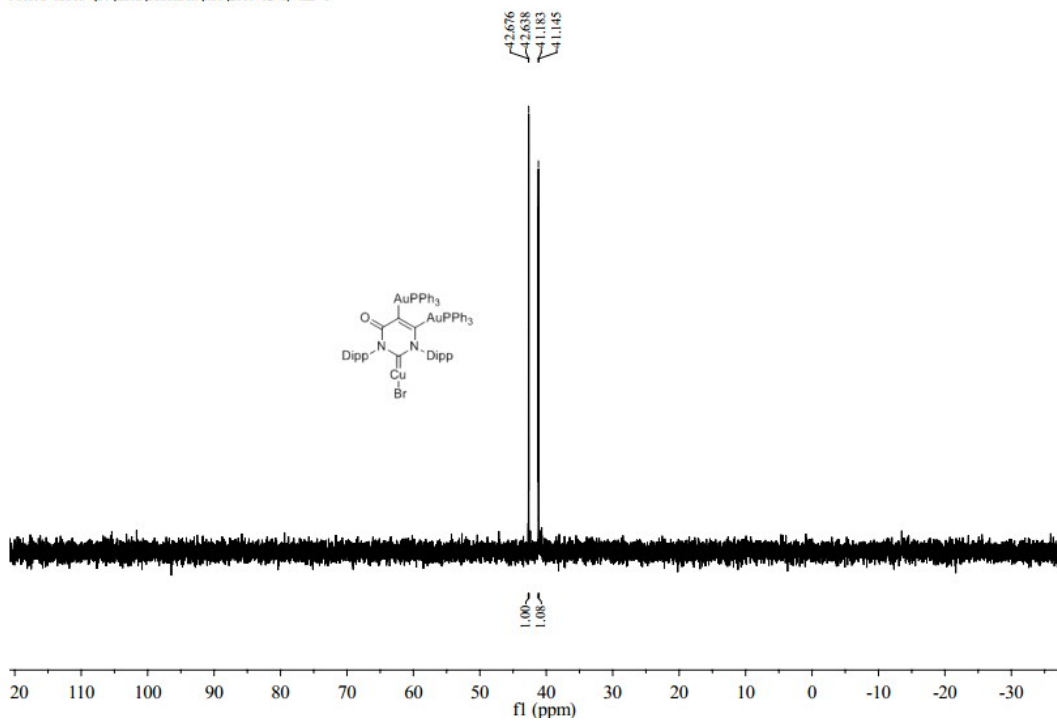
ju-chn-7341
P31CPD CDCl3 (D:\data\research\new\2017-1-3) nmr 18



Complex 4

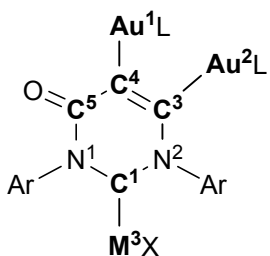


ju-zf-505
F31CPD CDC13 [D:\data\research\new\2016-12-8} nmr 1



Computational Details

Gaussian 09 suite of program² was employed for all the density functional theory (DFT) calculations utilizing the TPSS functional^{3,4} with Grimme's D3-BJ⁵ correction in combination with the triple- ζ basis set def2-TZVPP.^{6,7} Solvent corrections were based on the integral equation formalism version of polarizable continuum model (IEF-PCM)⁸⁻¹⁰ for 1,2-dichloroethane ($\epsilon = 10.125$) during the geometries optimization of the complexes. This theoretical methodology has recently been validated to yield good structural parameters for Au-carbene complexes.¹¹⁻¹³



M = Au(**2**), Ag(**3**), Cu(**4**); L = PPh₃

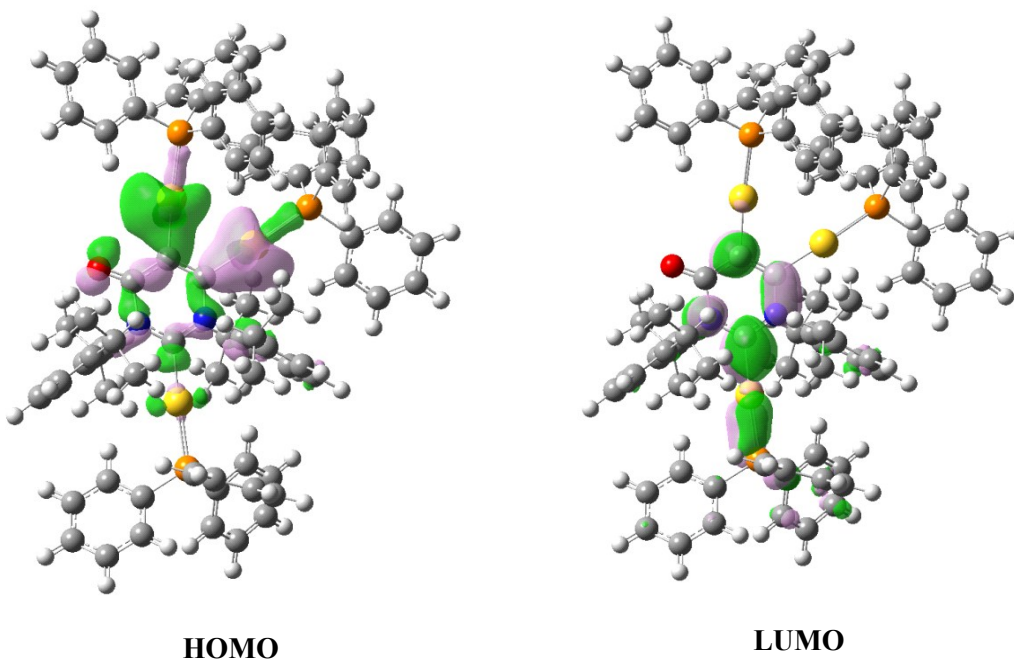
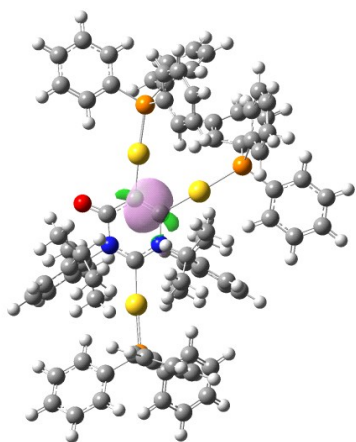
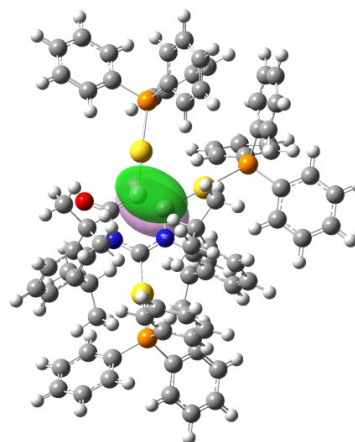


Figure S1: HOMO and LUMO orbitals of complex **2**.



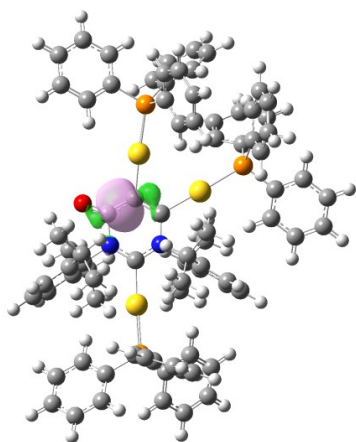
$$0.7041(sp^{1.67})_{C3} + 0.7101(sp^{1.50})_{C4}$$

σ bond



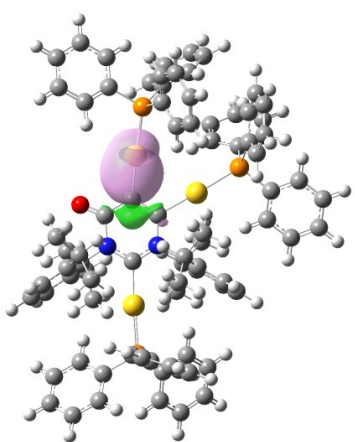
$$0.6821(p)_{C3} + 0.7313(p)_{C4}$$

π bond



$$0.7183(sp^{1.50})_{C5} + 0.6958(sp^{2.09})_{C4}$$

σ bond



$$0.5335(sp^{0.03}d^{0.19})_{Au1} + 0.8458(sp^{2.63})_{C4}$$

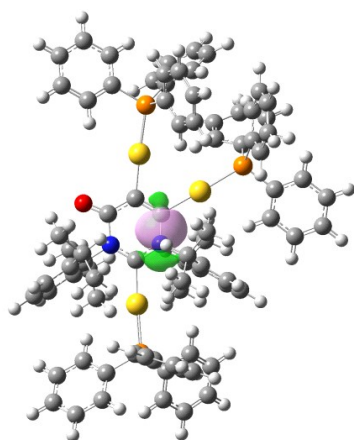
σ bond

Figure S2: All the NBOs of bonding and lone pair including C4 at the most stable Lewis structure of complex **2**. The NBO of coordinative bond between C4 and Au1 is identified, mainly composed of C4 hybrid orbital.



$$0.7041(sp^{1.67})_{C3} + 0.7101(sp^{1.50})_{C4}$$

σ bond



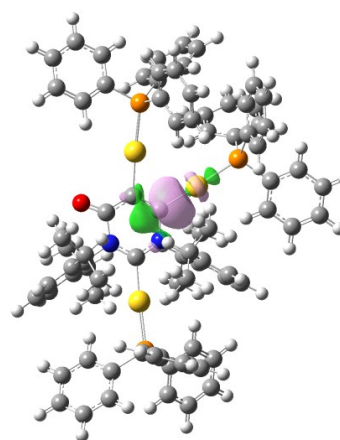
$$0.8122(sp^{1.88})_{N2} + 0.5833(sp^{2.50})_{C3}$$

σ bond



$$0.6821(p)_{C3} + 0.7313(p)_{C4}$$

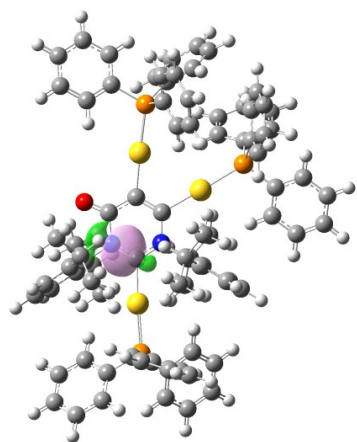
π bond



$$(sp^{1.95})_{C3}$$

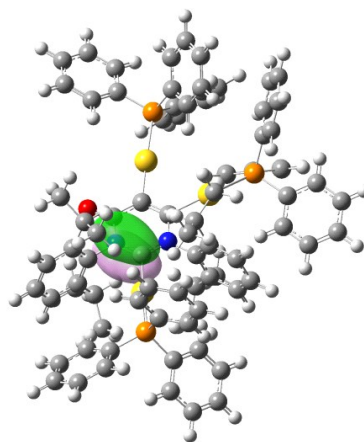
coordinative bond

Figure S3: All the NBOs of bonding and lone pair including C3 at the most stable Lewis structure of complex **2**. The NBO of coordinative bond between the lone pair of carbene C3 and Au2 is identified.



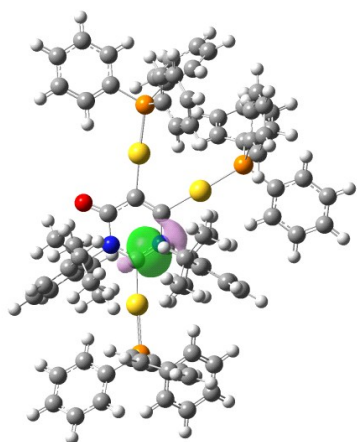
$$0.8006 (sp^{1.69})_{N1} + 0.5991(sp^{2.30})_{C1}$$

σ bond



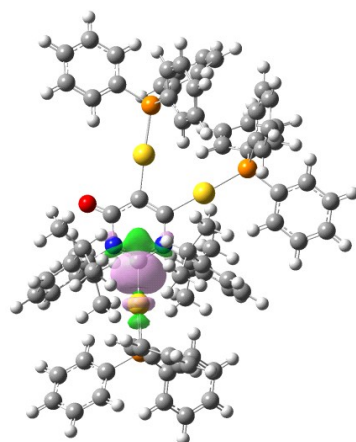
$$0.8730(p)_{N1} + 0.4878(p)_{C1}$$

π bond



$$0.8018(sp^{1.87})_{N2} + 0.5976(sp^{2.20})_{C1}$$

σ bond



$$(sp^{1.60})_{C1}$$

coordinative bond

Figure S4: All the NBOs of bonding and lone pair including C1 at the most stable Lewis structure of complex **2**. The NBO of coordinative bond between the lone pair of carbene C1 and Au3 is identified.

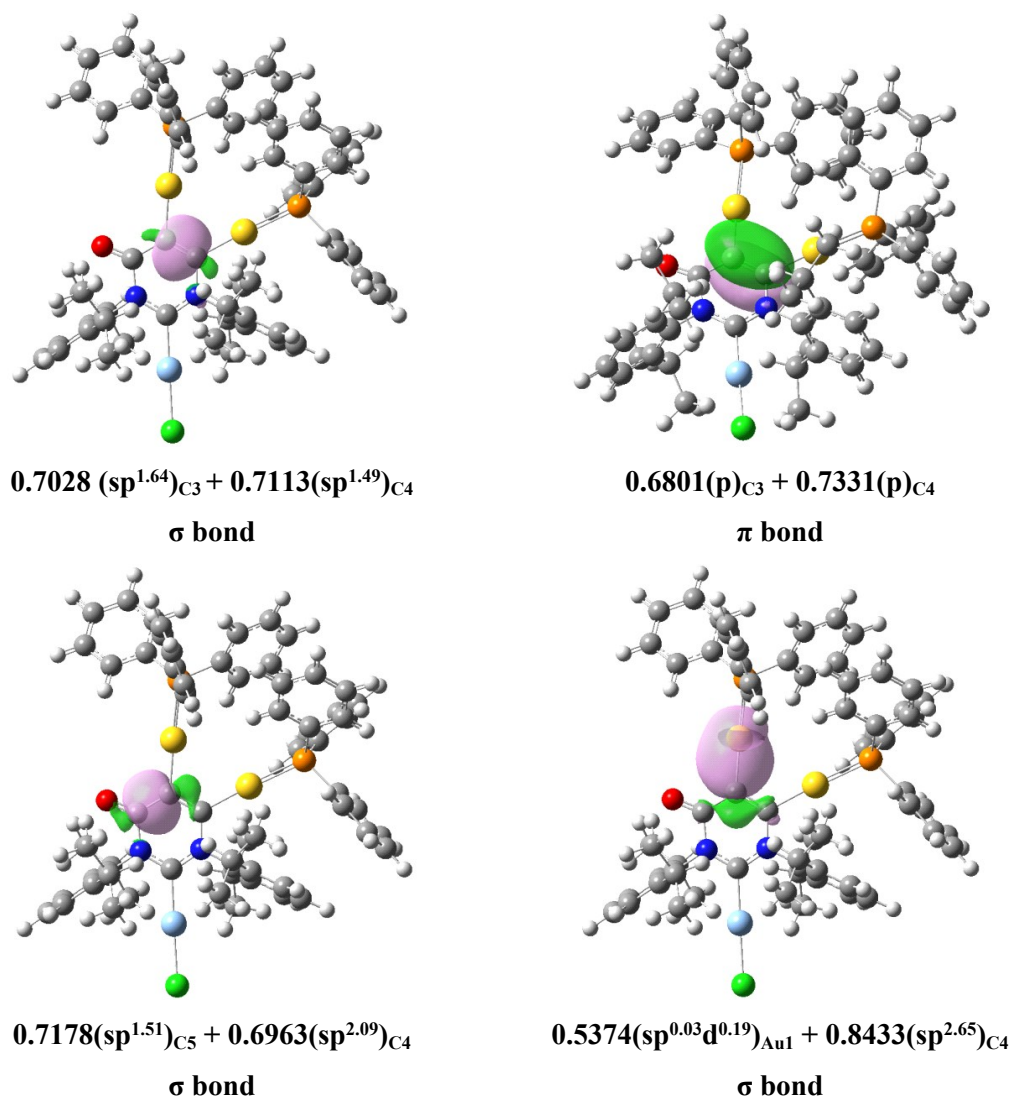
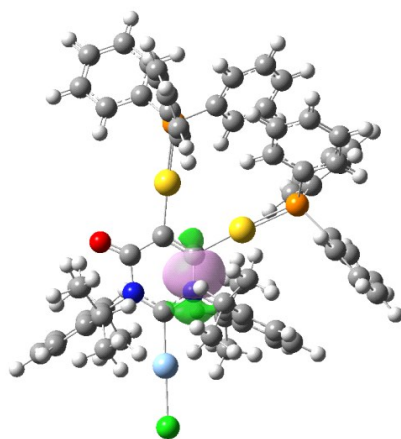


Figure S5: All the NBOs of bonding and lone pair including C4 at the most stable Lewis structure of complex **3**. The NBO of coordinative bond between C4 and Au1 is identified, mainly composed of C4 component.



$$0.7028(sp^{1.64})_{C3} + 0.7113(sp^{1.49})_{C4}$$

σ bond



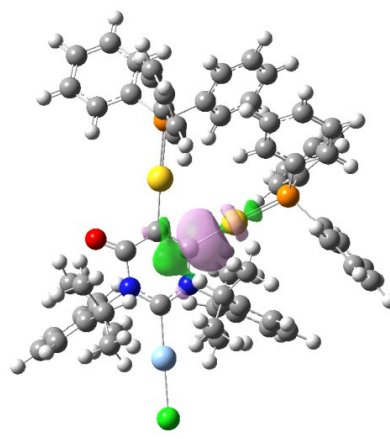
$$0.8114(sp^{1.64})_{N2} + 0.5845(sp^{1.49})_{C3}$$

σ bond



$$0.6801(p)_{C3} + 0.7331(p)_{C4}$$

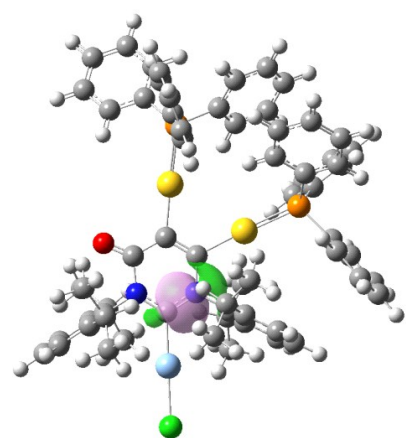
π bond



$$(sp^{1.98})_{C3}$$

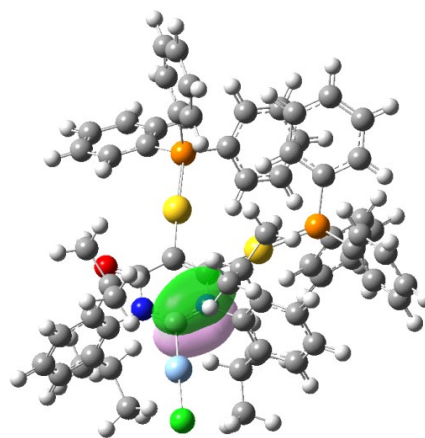
coordinative bond

Figure S6: All the NBOs of bonding and lone pair including C3 at the most stable Lewis structure of complex **3**. The NBO of coordinative bond between the lone pair of carbene C3 and Au2 is identified.



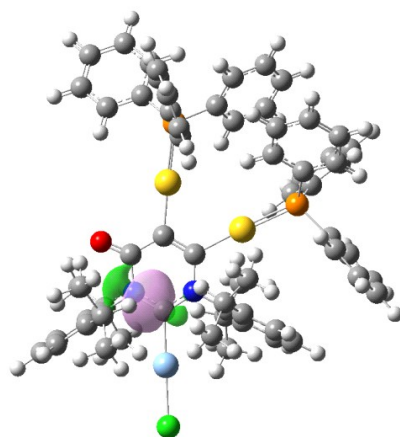
$$0.8077 (sp^{1.83})_{N2} + 0.5896(sp^{2.27})_{C1}$$

σ bond



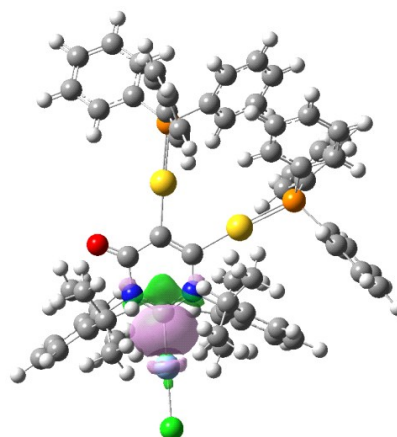
$$0.8779(p)_{N2} + 0.4788(p)_{C1}$$

π bond



$$0.8066(sp^{1.66})_{N1} + 0.5911(sp^{2.33})_{C1}$$

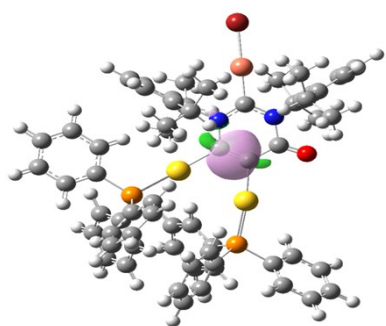
σ bond



$$(sp^{1.54})_{C1}$$

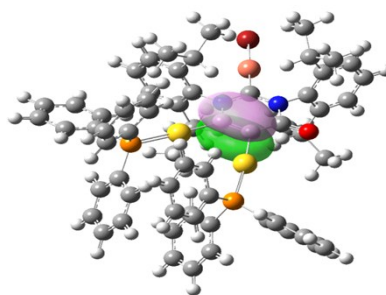
coordinative bond

Figure S7: All the NBOs of bonding and lone pair including C1 at the most stable Lewis structure of complex **3**. The NBO of coordinative bond between the lone pair of carbene C1 and Ag3 is identified.



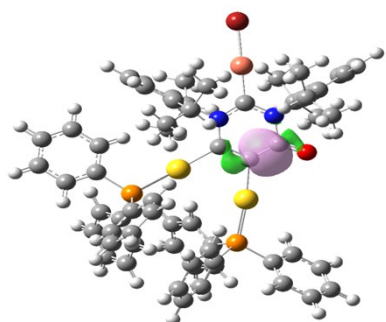
$$0.7032 (sp^{1.65})_{C3} + 0.7110(sp^{1.50})_{C4}$$

σ bond



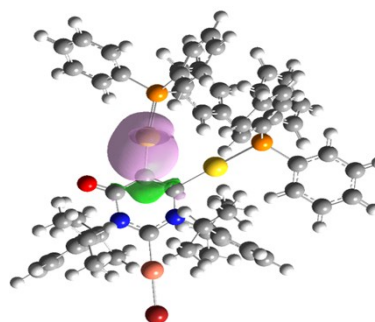
$$0.6791(p)_{C3} + 0.7340(p)_{C4}$$

π bond



$$0.7175(sp^{1.52})_{C5} + 0.6965(sp^{2.06})_{C4}$$

σ bond



$$0.5369(sp^{0.03}d^{0.19})_{Au1} + 0.8437(sp^{2.65})_{C4}$$

σ bond

Figure S8: All the NBOs of bonding and lone pair including C4 at the most stable Lewis structure of complex 4. The NBO of coordinative bond between C4 and Au1 is identified, mainly composed of C4 component.



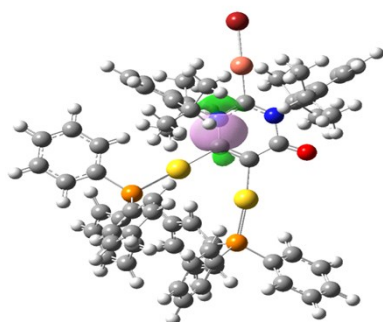
$$0.7032 (sp^{1.65})_{C3} + 0.7110(sp^{1.50})_{C4}$$

σ bond



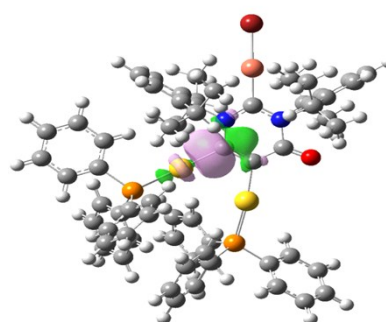
$$0.6791(p)_{C3} + 0.7340(p)_{C4}$$

π bond



$$0.8107(sp^{1.83})_{N2} + 0.5855(sp^{2.44})_{C3}$$

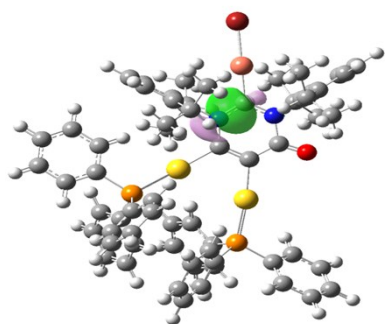
σ bond



$$(sp^{2.01})_{C3}$$

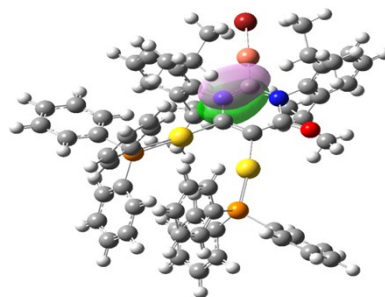
coordinative bond

Figure S9: All the bonding and lone pair NBOs of C3 at the most stable Lewis structure of complex 4. The coordinative bond between the lone pair of carbene C3 and Au2 is identified.



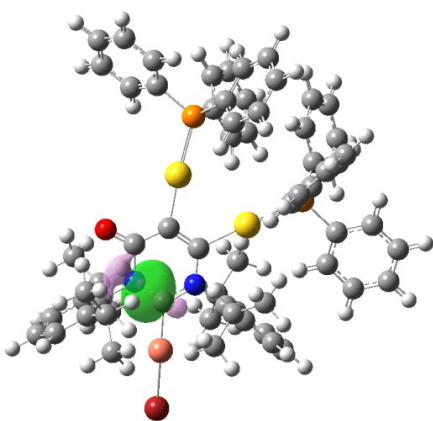
$$0.8039 (sp^{1.88})_{N2} + 0.5948(sp^{2.26})_{C1}$$

σ bond



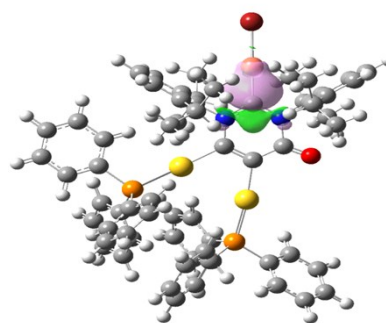
$$0.8788 (p)_{N2} + 0.4773(p)_{C1}$$

π bond



$$0.8032 (sp^{1.69})_{N1} + 0.5957(sp^{2.31})_{C1}$$

σ bond



$$(sp^{1.56})_{C1}$$

coordinative bond

Figure S10: All the NBOs of bonding and lone pair including C1 at the most stable Lewis structure of complex **4**. The NBO of coordinative bond between the lone pair of carbene C1 and Cu3 is identified.

X-Ray Crystallography.

Each crystal was mounted on a glass fiber. Crystallographic measurements were made on a Bruker Smart Apex 100 CCD area detector using graphite monochromated Mo-K α radiation ($\lambda_{\text{Mo-K}\alpha} = 0.71073 \text{ \AA}$). The structures were solved by direct methods (SHELXS-97) and refined on F^2 by full-matrix least squares (SHELX-97) using all unique data. All the calculations were carried out with the SHELXTL18 program.

Key details of the crystal and structure refinement data are summarized in Table S1-3. Further crystallographic details may be found in the respective CIF files, which were deposited at the Cambridge Crystallographic Data Centre, Cambridge, UK [CCDC 1528973 (**2**), CCDC 1528969 (**3**), and CCDC 1528970(**4**).

Table S1. Crystal Data, Data Collection, and Structure Refinement for **2**, **3** and **4**.

	2	3	4
Identification code	cu_dm16773_0m	mo_dm16818_0m	mo_dm16837_0m
Formula	C ₈₂ H ₇₉ Au ₃ N ₂ OP ₃	C ₇₀ H ₇₆ AgAu ₂ ClN ₂ O ₃ P ₂	C ₆₄ H ₆₄ Au ₂ BrCuN ₂ OP ₂
Formula weight	1792.28	1592.52	1476.49
<i>T</i> , K	130	130	130
crystal system	Monoclinic	Triclinic	Monoclinic
space group	P 1 21/c 1	P -1	P 1 21/c 1
<i>a</i> , Å	13.9827(9)	13.8956(12)	18.6441(15)
<i>b</i> , Å	14.8116(11)	16.1336(14)	14.8478(13)
<i>c</i> , Å	36.774(2)	16.6738(14)	24.590(2)
, deg	90	78.9410(10)	90
, deg	90.166(3)	78.141(2)	107.238(2)
, deg	90	65.151(2)	90
Volume, Å ³	7616.1(9)	3296.1(5)	6501.2(9)
<i>Z</i>	4	2	4
<i>D</i> _{calc} , Mg / m ³	1.563	1.605	1.509
absorption coefficient, mm ⁻¹	11.576	4.869	5.528
F(000)	3500	1572	2888
crystal size, mm	0.05 x 0.03 x 0.02	0.12 x 0.08 x 0.07	0.1 x 0.08 x 0.05
2θ range, deg	2.403 to 66.673	1.631 to 30.770	0.87 to 30.65
reflections collected /unique	37074/12906 [R(int) = 0.0692]	33851/20197 [R(int) = 0.0417]	66695/12760 [R(int) = 0.1063]
data / restraints/ parameters	12906 / 0 / 828	20197 / 0 / 742	12760 / 36 / 684
goodness of fit on F ²	1.043	0.969	1.027
final R indices [I > 2(I)] ^a	R1 = 0.0500, wR2 = 0.1367	R1 = 0.0427, wR2 = 0.0756	R1 = 0.0417, wR2 = 0.0861
R indices (all data)	R1 = 0.0588, wR2 = 0.1437	R1 = 0.0803, wR2 = 0.0866	R1 = 0.0735, wR2 = 0.0972
lgst diff peak and hole, e/Å ³	1.642 and -1.898	2.333 and -1.360	1.031 and -1.727

Supplementary References:

1. Chen, H. *et al.* Catalytic domino amination and oxidative coupling of gold acetylides and isolation of key vinylene digold intermediates as a new class of ditopic N-heterocyclic carbene complexes. *Chem. Commun.* 2017, **53**, 10835.
2. M. J. Frisch, G. W. Trucks, H. B. Schlegel, G. E. Scuseria, M. A. Robb, J. R. Cheeseman, G. Scalmani, V. Barone, B. Mennucci, G. A. Petersson, H. Nakatsuji, M. Caricato, X. Li, H. P. Hratchian, A. F. Izmaylov, J. Bloino, G. Zheng, J. L. Sonnenberg, M. Hada, M. Ehara, K. Toyota, R. Fukuda, J. Hasegawa, M. Ishida, T. Nakajima, Y. Honda, O. Kitao, H. Nakai, T. Vreven, J. A. Montgomery, Jr., J. E. Peralta, F. Ogliaro, M. Bearpark, J. J. Heyd, E. Brothers, K. N. Kudin, V. N. Staroverov, R. Kobayashi, J. Normand, K. Raghavachari, A. Rendell, J. C. Burant, S. S. Iyengar, J. Tomasi, M. Cossi, N. Rega, J. M. Millam, M. Klene, J. E. Knox, J. B. Cross, V. Bakken, C. Adamo, J. Jaramillo, R. Gomperts, R. E. Stratmann, O. Yazyev, A. J. Austin, R. Cammi, C. Pomelli, J. Ochterski, R. L. Martin, K. Morokuma, V. G. Zakrzewski, G. A. Voth, P. Salvador, J. J. Dannenberg, S. Dapprich, A. D. Daniels, O. Farkas, J. B. Foresman, J. V. Ortiz, J. Cioslowski and D. J. Fox, Gaussian 09 (Revision D.01), Gaussian, Inc., Wallingford, CT, 2009.
3. Tao, J., Perdew, J. P., Staroverov, V. N. & Scuseria, G. E. Climbing the density functional ladder: nonempirical meta-generalized gradient approximation designed for molecules and solids. *Phys. Rev. Lett.* 2003, **91**, 146401.
4. Weigend, F. & Ahlrichs, R. Balanced basis sets of split valence, triple zeta valence and quadruple zeta valence quality for H to Rn: design and assessment of accuracy. *Phys. Chem. Chem. Phys.* 2005, **7**, 3297.
5. Weigend, F. Accurate coulomb-fitting basis sets for H to Rn. *Phys. Chem. Chem. Phys.* 2006, **8**, 1057.
6. Grimme, S., Antony, J., Ehrlich, S. & Krieg, H. A consistent and accurate ab initio parametrization of density functional dispersion correction (DFT-D) for the 94 elements H-Pu. *J. Chem. Phys.* 2010, **132**, 154104.
7. Grimme, S., Ehrlich, S. & Goerigk, L. Effect of the damping function in dispersion corrected density functional theory. *J. Comput. Chem.* 2011, **32**, 1456.
8. Miertuš, S., Scrocco, E. & Tomasi, J. Electrostatic interaction of a solute with a continuum. A direct utilization of AB initio molecular potentials for the prevision of solvent effects. *Chem. Phys.* 1981, **55**, 117.
9. Barone, V. & Cossi, M. Quantum calculation of molecular energies and energy gradients in solution by a conductor solvent model. *J. Phys. Chem. A* 1998, **102**, 1995.

10. Cossi, M. & Barone, V. Separation between fast and slow polarizations in continuum solvation models. *J. Phys. Chem. A* 2000, **104**, 10614.
11. Nava, P., Hagebaum-Reignier, D. & Humbel, S. Bonding of gold with unsaturated species. *ChemPhysChem* 2012, **13**, 2090.
12. Comprido, L. N. S., Klein, J. E. M. N., Knizia, G., Kästner, J. & Hashmi, A. S. K. The stabilizing effects in gold carbene complexes. *Angew. Chem. Int. Ed.* 2015, **54**, 10336.
13. Wang, J. *et al.* Synthesis and structures of gold and copper carbene intermediates in catalytic amination of alkynes. *Nat. Commun.* 2017, **8**, 14625.